24th INTERNATIONAL CONGRESS ON SOUND AND VIBRATION
23–27 July 2017, London

PREDICTION OF NOISE FROM MACHINERY IN TIMBER-FRAME BUILDINGS USING TRANSMISSION FUNCTIONS

Fabian Schöpfer, Andreas R. Mayr and Ulrich Schanda
Laboratory for Sound Measurement LaSM, University of Applied Sciences Rosenheim, Hochschulstr. 1, 83024 Rosenheim, Germany.
email: fabian.schoepfer@fh-rosenheim.de

Carl Hopkins
Acoustics Research Unit, School of Architecture, University of Liverpool, L69 7ZN, UK.

To ensure that building regulations are satisfied, the sound pressure level due to machinery has to be predicted at the design stage of a new building. With the increasing popularity of multi-story timber dwellings, prediction becomes an important issue for designers and consultants. At present previous project experience is often used when considering the design of wall and floor constructions and the mounting positions for machinery. Simple tools to calculate the sound pressure levels in rooms based on machinery data and construction details are not currently available. The approach involves two stages: firstly the description of the source and secondly the prediction of vibration transmission across the building and sound radiation into the rooms. In this paper a simple empirical model is proposed for the second stage. This approach is based on measured transmission functions that are defined as the average sound pressure level in a receiving room relative to the injected structure-borne sound power. This is a logical extension of approaches to characterize structure-borne sound sources that also use a power based descriptor (e.g. prEN 15657:2016-02: *Acoustic properties of building elements and of buildings - Laboratory measurement of structure-borne sound from building service equipment for all installation conditions*) and provides a simple method to estimate the sound pressure level in a room.

Keywords: Structure-borne sound, transmission, timber-frame buildings

1. Introduction

The EN 12354-5 model [1] is primarily intended for heavyweight buildings and for receiving rooms that are horizontally-, vertically- or diagonally-adjacent to the source room which contains the machinery. The extension of the scope of this standard to lightweight constructions requires an adaptation of the methods to cope with more complex description of sound transmission in framed constructions. A potential approach is to use transmission functions which quantify the combination of all transmission paths. This quantity is expected to be unique for a specific situation, whereas predictive approaches like the model described in EN 12354-5 are more general. However it is possible that different construction types could be grouped and an average transmission function could adequately predict sound pressure levels. For this reason transmission functions could provide a simplified calculation technique for consultants and manufacturers.

Mechanical-acoustical transfer functions have previously been investigated by Steenhoek, Ten Wolde and Verheij [2, 3] to describe the excitation of a strucure-borne sound source by reciprocity, including all six degrees-of-freedom. Later Buhlert and Feldmann [4], Vercammen and Heringa [5], Gerretsen [6], Fischer [7] as well as Kornadt, Arnold, Wittstock and Scholl [8, 9] proposed methods based on transfer functions to predict machinery noise in buildings based on the ratio between sound pressure and applied force. A method to measure the total transmission from force excitation to sound pressure is also described in Annex F of EN 12354-5:2009.

In this paper a transmission function is proposed that relates the spatial-average sound pressure level in a room to the structure-borne sound power level injected into a building element [10]. Using a descriptor that includes the installed power is aligned with standardized methods for source characterisation like prEN 15657 [11] and SEA-based prediction models like EN 12354-5. Since machinery tends to inject high levels of structure-borne sound power at low frequencies [12, 13, 14], the frequency range was extended down to the $20\,\mathrm{Hz}$ one-third octave band, following a low-frequency procedure described in [15, 16, 17]. Using the protocol described in section 2, a survey was conducted to collect data for various timber constructions in the laboratory and in the field including horizontal, diagonal and vertical transmission as well as transmission to non-adjacent rooms. Further, the application of transmission functions to predict machinery noise is presented in case studies with an idealized as well a real structure-borne sound source.

2. Proposed methodology to determine transmission functions

The injected narrow-band power $W_{\mathrm{NB},k}$, at an excitation position, k, is calculated from the real part of the cross-spectrum of the force and velocity.

$$W_{\mathrm{NB},k} = \frac{1}{2}\,\mathrm{Re}\left\{\underline{\hat{F}}\,\underline{\hat{v}}^{*}\right\} \tag{1}$$

where $\underline{\hat{F}}$ is the complex peak force and $\underline{\hat{v}}^{*}$ is the complex conjugate peak velocity. The power in decibels in one-third octave bands $L_{\mathrm{W},k}$ at excitation point k is calculated according to

$$L_{W,k} = 10\lg\left(\frac{\sum_{j=1}^{J} W_{\mathrm{NB},k,j}}{W_0}\right) \tag{2}$$

where $W_{\mathrm{NB},k,j}$ is the injected power for narrow-band j at excitation position k, W_0 is the reference structure-borne sound power of 10^{-12} W, and J is the number of narrow bands that form the one-third octave band.

For each excitation position k, the sound pressure is measured in narrow bands using various microphone positions i. The narrow band autospectrum is converted into one-third octave bands using

$$p_{i,k}^2 = \sum_{j=1}^{J} \tilde{p}_{\mathrm{NB},i,j,k}^2 \tag{3}$$

where $\tilde{p}_{\mathrm{NB},i,j,k}$ is the root mean square pressure for narrow band j. For each microphone position i the one-third octave band sound pressure levels are corrected for background noise.

The spatial-average sound pressure level, $L_{\mathrm{av},k}$ for M microphone positions is determined by

$$L_{\mathrm{av},k} = 10\lg\left(\frac{\sum_{i=1}^{M} \tilde{p}_{i,k,\mathrm{corr}}^2}{M\,p_0^2}\right) \tag{4}$$

where $\tilde{p}_{i,k,\mathrm{corr}}^2$ is the one-third octave band mean-square pressure at position i with excitation position k corrected for background noise and p_0 is the reference sound pressure of $2\times10^{-5}\,\mathrm{Pa}$. If required, a correction for possible airborne flanking transmission can be applied to the spatial-average sound pressure level, $L_{\mathrm{av},k}$.

To determine the spatial-average sound pressure level at low frequencies the procedure for field measurements of sound insulation [15] can be applied as described in [10]. As previous work showed

[18, 19], this can be used down to the $20\,\mathrm{Hz}$ one-third octave band for room volumes ranging from $18\,\mathrm{m}^3$ to $245\,\mathrm{m}^3$, which can be particularly important for machinery noise.

Using the spatial-average sound pressure level, $L_{\mathrm{av},k}$ and the level of the injected power $L_{W,k}$, the transmission function $D_{\mathrm{TF},k}$ for an excitation point, k, is defined by

$$D_{\mathrm{TF},k} = L_{\mathrm{av},k} - L_{W,k} \tag{5}$$

This transmission function can be spatially averaged for K excitation positions to give an average transmission function, $D_{\mathrm{TF,av}}$ by

$$D_{\mathrm{TF,av}} = 10\lg\left(\frac{\sum_{k=1}^{K} 10^{0.1 D_{\mathrm{TF},k}}}{K}\right) \tag{6}$$

The standardized spatial-average transmission function, $D_{\mathrm{TF,av,n}T}$ is then given by

$$D_{\mathrm{TF,av,n}T} = D_{\mathrm{TF,av}} - 10\lg\left(\frac{T}{T_0}\right) \tag{7}$$

where T is the reverberation time in the receiving room and T_0 is the reference reverberation time of $0.5\,\mathrm{s}$. Similarily the absorption area can be used to get a normalized spatial-average transmission function.

3. Survey of measured transmission functions

At present there is a lack of validated prediction models for the transmission of structure-borne sound caused by machinery in timber-frame constructions. Some data sets are available from previous work (e.g. [5, 8, 9]), but only for direct transmission to either vertically- or horizontally-adjacent rooms. Using the protocol described in section 2 a field survey was carried out to determine transmission functions in timber-frame constructions.

3.1 Field measurements

In the field study, transmission functions were measured in seven timber-frame buildings to horizontally-, vertically- and diagonally-adjacent rooms as well as non-adjacent rooms. A total of 34 average transmission functions were determined in detached houses, guesthouses and apartment buildings. Only walls were excited because every building had a floating floor. At least two excitation positions were taken into account, one position was above, or close to a stud and one was in a bay. This allowed calculation of an average transmission function to cover both situations. In all situations transient excitation was used, except for transmission to non-adjacent rooms where steady-state excitation was used in addition to the force hammer. In all cases the power input was measured by using a pair of accelerometers next to the excitation point following the procedure that was validated and described in [10]. Measurements were performed in unoccupied buildings during the construction phase. To ensure measurements were taken in completed buildings with minimal construction noise and without airborne flanking due to missing doors, the measurements were scheduled just before transfer to the owner when all the main construction work had been completed. The transmission functions were calculated according to equation (7) at and above the $50\,\mathrm{Hz}$ one-third octave band. Below $50\,\mathrm{Hz}$ equation (6) was used.

3.2 Results

In Figures 1 (a) - 1 (f) the measured data is grouped in terms of the direction of transmission and the type of construction. These data give initial insights into the range of transmission functions that

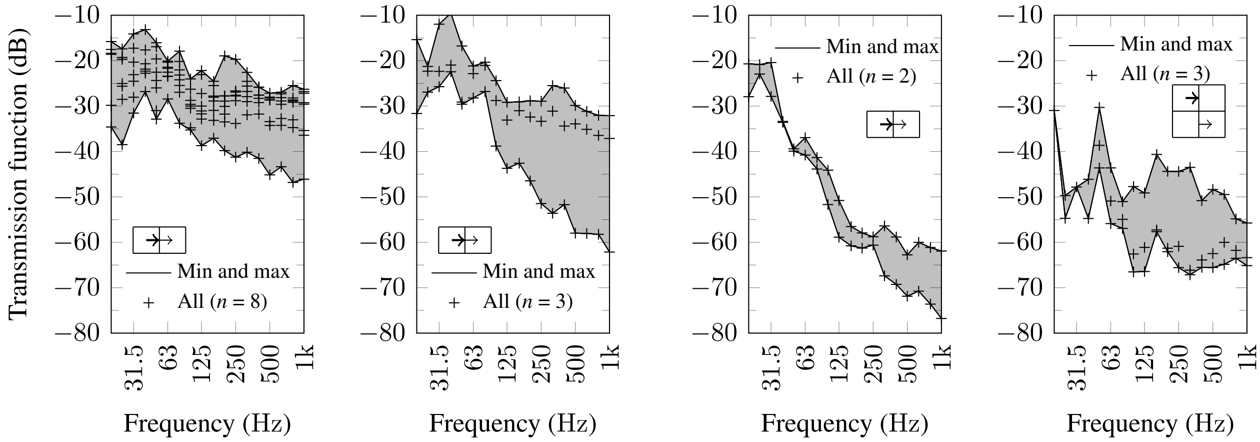

(a) Timber-frame single wall with plasterboard on both sides, horizontal transmission.

(b) Like (a), but with additional plasterboard lining (e.g for pipework), horizontal transmission.

(c) Timber-frame double wall with individual frames (party wall), horizontal transmission.

(d) Timber-frame single wall with plasterboard on both sides, diagonal transmission.

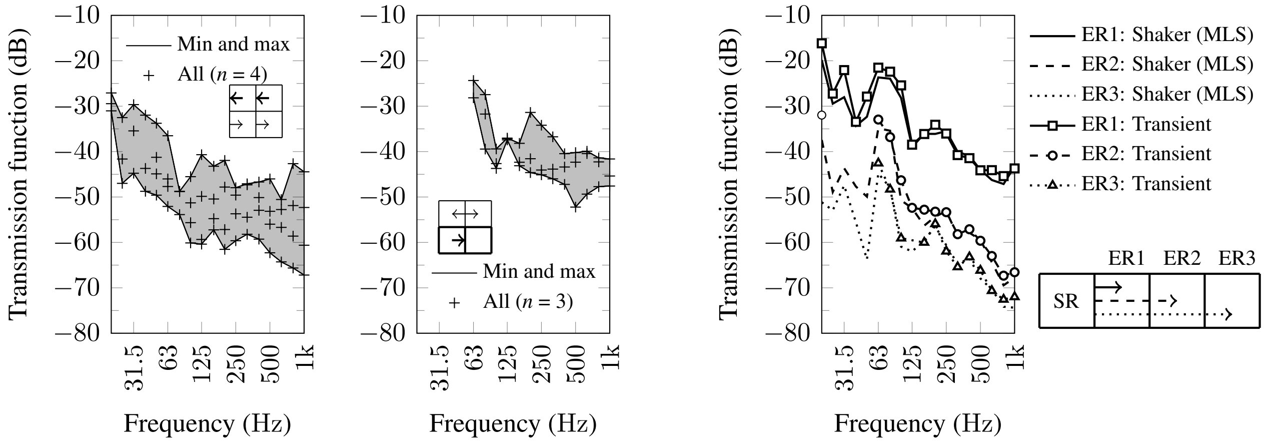

(e) Interior and exterior timber-frame walls (single and double), vertical transmission.

(f) Heavyweight wall in basement to timber-frame wall on the ground floor, vertical and diagonal transmission.

(g) Transmission to adjacent and non-adjacent rooms, using transient and steady-state excitation. Timber-frame single wall with additional battens on resilient mounts perpendicular to the wall studs.

Figure 1: Survey of transmission functions measured in the field.

exist in typical timber-frame buildings. The spread of results within groups of similar constructions and transmission direction is up to 20 dB. However the available dataset is relatively small; hence future work will need to collect more data in order to form more detailed groups to try and reduce the variation.

Figure 1g shows transmission functions to non-adjacent rooms measured with transient as well as steady-state excitation. These results show the reduction of transmission across successive receiving rooms in a timber-frame building which means that it is not always possible to take measurements using transient excitation.

The average transmission functions in Figures 1 (a) - 1 (f) are determined using at least two excitation positions to account for significant differences in the driving point mobility that can occur in framed constructions (e.g. see [20]). As an example, Figure 2 (a) shows the driving point mobilities of a basic construction formed by a single framework with a single layer of chipboard in the laboratory for positions above studs and positions in bays. Following these findings, at least one position was chosen in a bay and another above or close to a stud in the field although there was some uncertainty due to the finished surface obscuring the exact positions of the studs. Figure 2 (b) shows the spatial

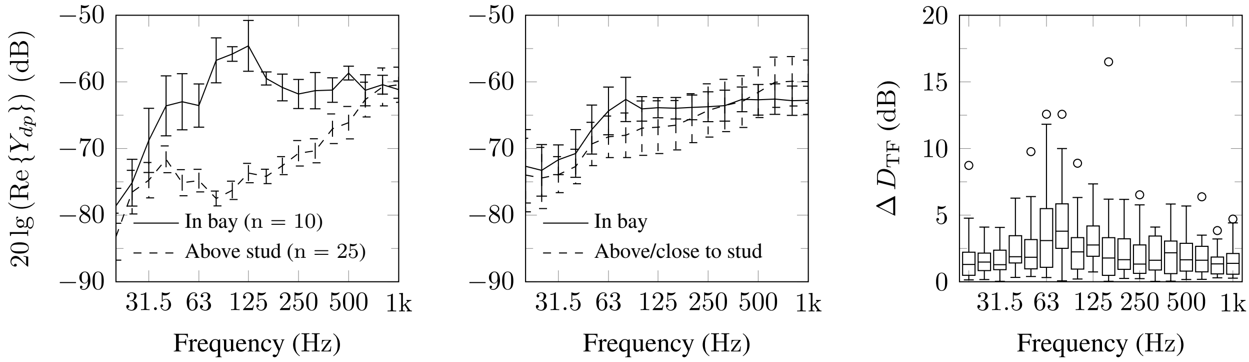

(a) Spatial variation of driving-point mobilities for the basic laboratory construction. Mean values with 95 % confidence limits. Bay positions: n = 10, Stud positions: n = 25.

(b) Spatial variation of driving-point mobilities in the field. Mean values with 95 % confidence limits. Bay positions: n = 11, Stud positions: n = 14.

(c) Differences between the maximum and minimum value for D_{TF} determined for every transmission situation with at least two excitation positions in the field.

Figure 2: Influence of the excitation position on the driving point mobility and and the transmission function.

variation of mobilities determined in the field. The variation is smaller compared to the laboratory due to double layers of plasterboard and the uncertainty in finding the exact stud positions as mentioned above. The influence of the excitation position on the transmission function is shown in Figure 2 (c) in terms of the difference between the maximum and minimum in every transmission situation. The upper quartile (75 %) of the differences between the excitation positions is up to 6 dB in the 63 Hz and 80 Hz one-third octave band, where the driving point mobilities also differ most (see Figure 2 (b)). However the difference is ≈ 3 dB on average for the frequency range from 20 Hz to 1000 Hz.

4. Case studies

In this section the application of transfer functions to the prediction of machinery noise is investigated for two multi-contact structure-borne sound sources. These were an idealized source (steel frame, driven by an inertial shaker) and a ventilation unit - see Figure 3. The approach involves two stages, the description of the source including the coupling to the structure and the description of the transmission, which is covered by the transmission function.

(a) Idealized source

(b) Ventilation unit

Figure 3: Structure-borne sound sources.

4.1 Structure-borne sound source characterization

To determine the power injected into the structure, three quantities are needed: (a) The source activity (e.g. the free velocity), (b) the source mobility and (c) the mobility of the receiver (e.g. see [21]). For a single point the power input can be calculated according to equation (8).

$$W_{\text{NB,sp}} = \frac{1}{2} \frac{|\hat{\underline{v}}_{\text{Sf}}|^2}{|\underline{Y}_{\text{S}} + \underline{Y}_{\text{R}}|^2} \cdot \text{Re}\{\underline{Y}_{\text{R}}\} \tag{8}$$

where $\hat{\underline{v}}_{\text{Sf}}$ is the free velocity and $\underline{\text{Y}}_{\text{S}}$ and $\underline{\text{Y}}_{\text{R}}$ are source and receiver mobilities respectively.

For multi-point sources these quantities must be available for every contact point, including the phase information. To account for interactions between the contact points the complex transfer mobilities are required to calculate the input power according to equation (9), where $\{\hat{\underline{v}}_{\text{Sf}}\}$ is the vector of free velocities and $\underline{\mathbf{Y}}_{\text{S}}$ and $\underline{\mathbf{Y}}_{\text{R}}$ are the mobility matrices of the source and the receiver.

$$\underline{W}_{\text{NB,mp}} = \frac{1}{2} \{\hat{\underline{v}}_{\text{Sf}}\}^{\text{T}} \, \underline{\mathbf{Y}}_{\text{R}}^{\text{T}} \, [\underline{\mathbf{Y}}_{\text{S}} + \underline{\mathbf{Y}}_{\text{R}}]^{-1^{\text{T}}} \, [\underline{\mathbf{Y}}_{\text{S}}^{*} + \underline{\mathbf{Y}}_{\text{R}}^{*}]^{-1} \, \{\hat{\underline{v}}_{\text{Sf}}\}^{*} \tag{9}$$

The source quantities were measured in the laboratory approximating free conditions using rubber cords. For both sources the full set of point and transfer mobilities was determined but only perpendicular forces were taken into account. Moments and in-plane forces were neglected.

The receiver mobilities were measured in the transmission situations described in the following section. The input power was calculated using three different approaches including two steps of simplification. In (A) the power input was calculated according to equation (9) using full mobility matrices and the vector of free velocities. In (B) the power input was also calculated according to equation (9), but the transfer mobilities were neglected. In (C) the power input was calculated according to equation (8) using the sum of free velocities, averaged magnitudes of point mobilities for the source and a constant value of $1 \times 10^{-3}\,\text{m}/(\text{N s})$ for the receiver mobility.

4.2 Transmission situations

The idealized source was mounted for a horizontal transmission situation in the field, whereas the ventilation unit was in a laboratory test rig. In both situations the average transmission function was determined by averaging stud and bay positions. In the field situation two excitation positions were used, in the laboratory 17. The idealized source was screwed to studs at all four contact points. The contact points on the ventilation unit included both stud and bay positions. With the sources in operation, the sound pressure level was measured in the receiving room at various fixed microphone positions. The sound pressure level was corrected for background noise and airborne flanking where necessary.

4.3 Results

Figure 4 shows the comparison of measured sound pressure levels and the prediction for both situations. There are differences up to approximately $\pm\,10\,\text{dB}$. On average all approaches (A), (B) and (C) showed close agreement with the measured sound pressure level down to $20\,\text{Hz}$.

5. Conclusions

An empirical approach based on transmission functions provides a practical method to predict machinery noise in timber-frame constructions. Field data collected to-date gives insights into the range of transmission functions that are likely to occur with different timber frame constructions. However more field data is needed to identify average transmission functions for consultants, architects or manufactures and to give an indication of the uncertainty. Two case studies with different machinery

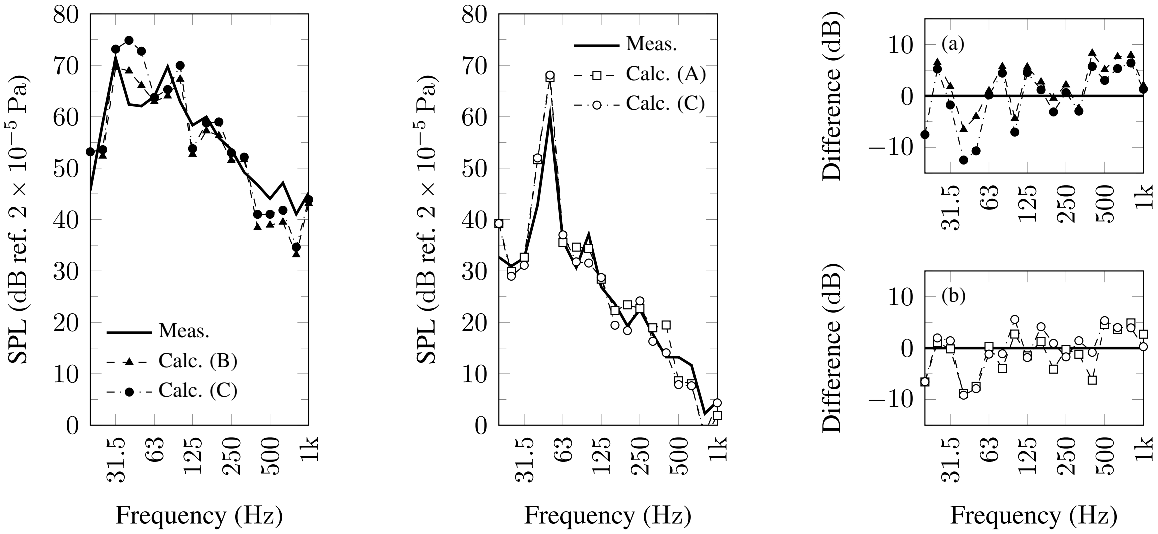

(a) Measured and predicted sound pressure level of the idealized source for horizontal transmission in the field.

(b) Measured and predicted sound pressure level of the ventilation unit for horizontal transmission in the laboratory test-rig.

(c) Difference between measured and predicted sound pressure level for (a) the idealized source in the laboratory and (b) the ventilation unit in the field

Figure 4: Results of the case studies. Calculation (A): power input acc. to eq. (9), full mobility matrices and the vector of free velocities; Calculation (B): power input acc. to eq. (9), transfer mobilities neglected; Calculation (C): power input acc. to eq. (8), sum of free velocities, averaged magnitudes of point mobilities for the source and constant value of $1 \times 10^{-3}\,\mathrm{m/(N\,s)}$ for the receiver mobility.

indicate that by considering only perpendicular forces (neglecting moment excitation) it is possible to accurately predict the sound pressure level between $20\,\mathrm{Hz}$ and $1\,\mathrm{kHz}$. For practical implementation it would also be useful to have a catalogue of structure-borne sound power data for machinery.

Acknowledgments

The authors gratefully acknowledge the cooperation with the industrial partners involved the project *Nachhaltiger Schallschutz gebäudetechnischer Anlagen in energetisch optimierten Gebäuden*, especially Regnauer Fertigbau GmbH and Stephan Lechner GmbH for the field measurements and Maico Elektroapparate-Fabrik GmbH for the ventilation unit. Special thanks also go to the colleagues from the HfT Stuttgart for the co-operational work related with the characterisation of the ventilation unit as well as to Katja Betz from the University of Applied Sciences Rosenheim for the support in the characterisation of the idealized source. This work was funded by the German Federal Ministry of Education and Research within the program FHProfUnt (Grant reference 03FH089PB2).

REFERENCES

1. EN 12354-5:2009. *Building acoustics – Estimation of acoustic performance of building from the performance of elements. Part 5: Sound levels due to the service equipment..*

2. Steenhoek, H. F. and Ten Wolde, T. The reciprocal mesurement of mechanical-acoustical transfer functions, *Acustica*, **23**, 301–305, (1970).

3. Ten Wolde, T., Verheij, J. W. and Steenhoek, H. F. Reciprocity method for the measurement of mechano-acoustical transfer functions, *Journal of Sound and Vibration*, **42** (1), 49–55, (1975).

4. von Buhlert, K.-J. and Feldmann, J. Ein Meßverfahren zur Bestimmung von Körperschallanregung und -übertragung, *Acustica*, **42** (3), 108–113, (1979).

5. Vercammen, M. L. S. and Heringa, P. H. Characterising structure-borne sound from domestic appliances, *Applied Acoustics*, **28**, 105–117, (1989).

6. Gerretsen, E. Estimation of air-borne and structure-borne sound transmission from machinery in buildings, *Applied Acoustics*, **40** (3), 255–265, (1993).

7. Fischer, H.-M. Determination and use of transfer functions to describe structure-borne sound transmission caused by equipment and installations, International Commission for Acoustics (Ed.), *Proceedings of the 17th International Congress on Acoustics, Rome, Italy*, (2001).

8. Kornadt, O., Arnold, J., Wittstock, V. and Scholl, W. Prediction of the sound pressure level caused by technical equipment in buildings by analyzing transfer functions, *Proceedings of Internoise 2012, 19-22-August, New York City, USA*, (2012).

9. Arnold, J. and Kornadt, O., (2014), Beschreibung Körperschallinduzierter Schalldruckpegel mit Hilfe von Übertragungsfunktionen. Fouad, N. A. (Ed.), *Bauphysik Kalender 2014*, pp. 641–663, Wiley-VCH Verlag GmbH.

10. Schöpfer, F., Hopkins, C., Mayr, A. R. and Schanda, U. Measurement of transmission functions in lightweight buildings for the prediction of structure-borne sound transmission from machinery, *Acta Acustica united with Acustica*, (accepted for publication in 2017).

11. prEN 15657:2016-02. *Acoustic properties of building elements and of buildings - Laboratory measurement of structure-borne sound from building service equipment for all installation conditions*.

12. Scheck, J. M., Reinhold, S., Eschbach, P. and Fischer, H.-M. Messung und Prognose der Luft- und Körperschallübertragung von gebäudetechnischen Anlagen im Massivbau, *Proceedings of DAGA 2016, 14-17 March, Aachen, Germany*, (2016).

13. Vogel, A., Arnold, J., Kornadt, O., Völker, C. and Wittstock, V. Prediction of sound pressure levels in rooms using EN 12354 and the characteristic structure-borne sound power of structure-borne sound sources, *Proceedings of Internoise 2016, 21-24 August, Hamburg, Germany*, (2016).

14. Mayr, A. R. and Gibbs, B. M. Approximate method for obtaining source quantities for calculation of structure-borne sound transmission into lightweight buildings, *Applied Acoustics*, **110**, 81–90, (2016).

15. ISO 16283-1:2014. *Acoustics – Field measurement of sound insulation in buildings and of building elements. Part 1: Airborne sound insulation*.

16. Hopkins, C. Revision of international standards on field measurements of airborne, impact and facade sound insulation to form the ISO 16283 series, *Building and Environment*, **92**, 703–712, (2015).

17. ISO 16032:2004. *Acoustics – Measurement of sound pressure level from service equipment in buildings – Engineering method*.

18. Hopkins, C. and Turner, P. Field measurement of airborne sound insulation between rooms with non-diffuse sound fields at low frequencies, *Applied Acoustics*, **66**, 1339–1382, (2005).

19. Simmons, C. Measurement of sound pressure levels at low frequencies in rooms. comparison of available methods and standards with respect to microphone positions, *Acta Acustica united with Acustica*, **85** (1), 88–100, (1999).

20. Mayr, A. R. and Gibbs, B. M. Point and transfer mobility of point-connected ribbed plates, *Journal of Sound and Vibration*, **330**, 4798–4812, (2011).

21. Petersson, B. A. T. and Gibbs, B. M. Towards a structure-borne sound source characterization, *Applied Acoustics*, **61**, 325–343, (2000).